

Statistical properties of twin beams generated in spontaneous parametric downconversion

Jan Peřina Jr.^{a,b*},
Ondřej Haderka^{a,b},
Martin Hamar^{a,b},

^a Joint Laboratory of Optics of Palacký University and
Institute of Physics of Academy of Sciences of the Czech Republic,
17. listopadu 50A, 772 00 Olomouc, Czech Republic

^b Department of Optics, Faculty of Natural Sciences, Palacký University,
17. listopadu 50, 772 00 Olomouc, Czech Republic

Measurement of photon-number statistics of fields composed of photon pairs generated in spontaneous parametric downconversion pumped by strong ultrashort pulses is described. Final detection quantum efficiencies, noises as well as possible loss of one or both photons from a pair are taken into account. Measured data provided by an intensified single-photon CCD camera are analyzed along the developed model. The joint signal-idler photon-number distribution is obtained using the expectation maximization algorithm. Covariance of the signal and idler photon-numbers equals 80 %. Statistics of the generated photon pairs are identified to be Poissonian in our case. Distribution of the integrated intensities of the signal and idler fields shows strong correlations between the fields. Negative values of this distribution occurring in some regions clearly demonstrate a nonclassical character of the light composed of photon pairs.

I. INTRODUCTION

Light generated in the process of spontaneous parametric downconversion is emitted in photon pairs [1]. Photons comprising one photon pair are strongly correlated — they are entangled. Entanglement of photons in a pair has been used in many experiments that have provided a deep insight into the laws of quantum mechanics [2,3]. Among others, the measured violation of Bell inequalities ruled out neoclassical local hidden-variables theories. Photon pairs have also found ways to practical applications, e.g., in quantum cryptography, measurement of ultrashort time delays, or absolute measurements of detection quantum efficiencies. These experiments utilized photon fields that contain only one photon pair in a measured time window with high probability.

There have been experiments (teleportation, measurement of GHZ correlations, etc.) measuring triple and quadruple coincidence counts caused by fields containing two photon pairs in the time window given by an ultrashort pump pulse during the last couple of years. However, states used for such experiments contain a very

low fraction of two photon-pair states in comparison with one photon-pair state and the vacuum state. The reason is to eliminate the influence of three and more-than-three photon-pair states in considered experimental setups. Measurements done in such setups are conditional and they require long data-acquisition times.

The use of more powerful pulses pump lasers as well as development of materials with higher values of $\chi^{(2)}$ susceptibilities open the way to generate fields containing more than one photon pair from one pump pulse with nonnegligible probabilities. For such fields, the influence of states containing two photon-pairs has to be judged even in experiments utilizing primarily just one photon pair. For example, the effect of two-photon-pair states in measurement of time-bin entanglement has been analyzed in [4]. Contribution from more-than-one photon-pair states becomes essential for higher mean values of photon pairs and such fields then have to be characterized in general by their photon-pair statistics.

Determination of photon-pair statistics is necessary also for characterization of weak continuous downconverted fields if they are detected in long time windows [5]. In this case photon-pair statistics were determined to be Poissonian if dead-time effects in their detection were eliminated [5].

We describe the behaviour of photon pairs in a general photon-number resolving system. Assuming detection of generated photon pairs by an intensified CCD camera, we can obtain a joint photon-number distribution of the signal and idler fields at the output plane of a crystal from measured data using a developed model of detection and a suitable reconstruction algorithm. The generated field can then be characterized in general by the joint distribution of the signal and idler integrated intensities.

The paper is organized as follows. Sec. 2 contains a general model describing a photon-number-resolving detection device. Sec. 3 is devoted to reconstruction of the joint signal-idler photon-number distribution. Joint signal-idler integrated-intensity distribution is determined in Sec. 4. Sec. 5 provides conclusions. Statistical properties of fields generated in spontaneous parametric downconversion are derived in Appendix A from first principles.

*e-mail: perina_j@sloup.upol.cz

II. MODEL DESCRIBING THE MEASUREMENT OF MULTIPHOTON-COINCIDENCE COUNTS

Measurement of the joint signal-idler photon-number distribution can be in general described using the scheme shown in Fig. 1 [6–8].

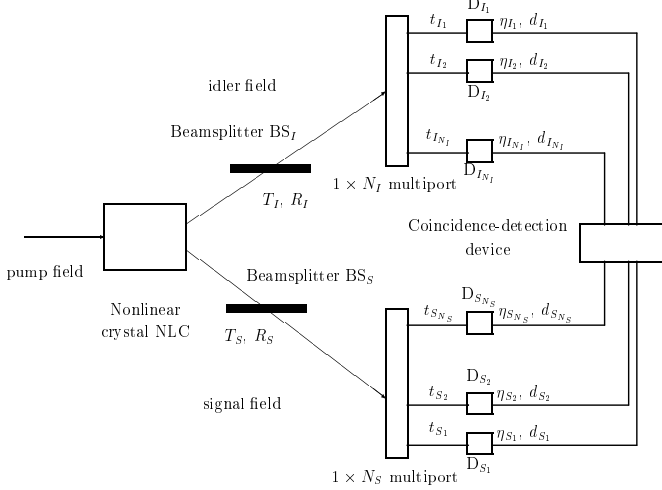


FIG. 1. Scheme of the considered model. Photon pairs are generated in nonlinear crystal NLC. Virtual beamsplitters BS_S and BS_I describe possible losses of one or both photons from a pair before they are detected. Signal (idler) photons propagate through a $1 \times N_S$ ($1 \times N_I$) multiport and are detected in single-photon detectors $D_{S_1}, D_{S_2}, \dots, D_{S_{N_S}}$ ($D_{I_1}, D_{I_2}, \dots, D_{I_{N_I}}$). Signals from the detectors are registered in a coincidence-detection device.

Photon pairs occurring in the output plane of nonlinear crystal NLC propagate towards photon-number-resolving detection devices. One or both photons from a pair may be lost before they reach their detection devices. The reasons may be geometric filtering (one photon from a photon pair is not collimated to the detector area), reflections on optical elements in experimental setup or absorption of a photon along its path to a detection device. We describe this effect by two beamsplitters BS_S and BS_I [9] placed in the signal-field and idler-field paths, respectively. We model a photon-number-resolving detection device as a multiport $1 \times N$ [10] followed by N single-photon detectors. This description is applicable also when an intensified CCD camera is used (as in our experiment). We note that detectors able to resolve directly photon numbers to some extent have been constructed [11–13]. From practical viewpoint, detectors using time multiplexing (reached in fiber optics) and one or two single-photon detectors are promising [14–16]. We note that an intensified CCD camera has already occurred to be useful when studying spatial correlations of photon pairs [17].

We assume that the signal and idler fields in the output plane of nonlinear crystal NLC are described by the following statistical operator $\hat{\rho}_{SI}$ written in Fock basis:

$$\hat{\rho}_{SI} = \sum_{n_S=0}^{\infty} \sum_{n_I=0}^{\infty} p(n_S, n_I) |n_S\rangle_{SS} \langle n_S| \otimes |n_I\rangle_{II} \langle n_I|; \quad (1)$$

the symbol $p(n_S, n_I)$ denotes the joint signal-idler photon-number distribution.

Statistical operator $\hat{\rho}_{SI}^D$ appropriate for the signal and idler fields in front of the detection devices can be written as:

$$\begin{aligned} \hat{\rho}_{SI}^D &= \sum_{n_S=0}^{\infty} \sum_{n_I=0}^{\infty} p(n_S, n_I) \\ &\times \sum_{l_S=0}^{n_S} \binom{n_S}{l_S} T_S^{l_S} R_S^{n_S-l_S} |l_S\rangle_{SS} \langle l_S| \\ &\times \sum_{l_I=0}^{n_I} \binom{n_I}{l_I} T_I^{l_I} R_I^{n_I-l_I} |l_I\rangle_{II} \langle l_I|. \end{aligned} \quad (2)$$

The symbols R_S and R_I (T_S and T_I) denote intensity reflectivities (transmissivities) of the beamsplitters in the signal-field and idler-field paths.

We assume a multiport $1 \times N_S$ ($1 \times N_I$) followed by N_S (N_I) single-photon detectors with quantum efficiencies η_{S_i} (η_{I_i}) and dark-count rates d_{S_i} (d_{I_i}) in the signal (idler) path. Detection of a photon in the k -th detector is described by the detection operator \hat{D}_k [6]:

$$\hat{D}_k = \sum_{n=0}^{\infty} \{ [1 - (1 - \eta_k)^n] + d_k (1 - \eta_k)^n \} |n\rangle_{kk} \langle n|. \quad (3)$$

Detection operator \hat{D}_k^{no} corresponds to the case when no detection has occurred:

$$\hat{D}_k^{\text{no}} = 1 - \hat{D}_k. \quad (4)$$

The effect of splitting photons in the signal field in a $1 \times N_S$ multiport can be described by the relation $\hat{a}_S = \sum_{i=1}^{N_S} t_{S_i} \hat{a}_{S_i}$, where \hat{a}_S is the annihilation operator of the signal field entering the multiport, the annihilation operator \hat{a}_{S_i} describes a field at the i -th multiport output, and t_{S_i} stands for amplitude transmissivity of a photon from the input to the i -th output. $1 \times N_I$ multiport in the idler-field path is described similarly and the symbol t_{I_i} then refers to amplitude transmissivity of a photon from the input to the i -th multiport output.

The probability C_{S^D, I^D} that given c_S detectors in the signal field and given c_I detectors in the idler field detect a photon whereas the rest of detectors does not register a photon is determined as follows:

$$\begin{aligned} C_{S^D, I^D} &= \text{Tr}_{SI} \left\{ \hat{\rho}_{SI}^D \prod_{a \in S^D} \hat{D}_a \prod_{b \in S \setminus S^D} \hat{D}_b^{\text{no}} \right. \\ &\times \left. \prod_{c \in I^D} \hat{D}_c \prod_{d \in I \setminus I^D} \hat{D}_d^{\text{no}} \right\}. \end{aligned} \quad (5)$$

The symbol S (I) denotes the set of all signal-field (idler-field) detectors $S = \{S_1, \dots, S_{N_S}\}$ ($I = \{I_1, \dots, I_{N_I}\}$). The set S^D (I^D) contains signal-field (idler-field) detectors that registered a photon.

Using the statistical operator $\hat{\rho}_{SI}^D$ in Eq. (2) the probability C_{S^D, I^D} defined in Eq. (5) is written in the form:

$$\begin{aligned}
C_{S^D, I^D} &= \sum_{n_S=0}^{\infty} \sum_{n_I=0}^{\infty} p(n_S, n_I) K_{S, S^D}(n_S) K_{I, I^D}(n_I), \\
K_{S, S^D}(n_S) &= (-1)^{c_S} \left[\prod_{b \in S} (1 - d_b) \right] \\
&\times \left[T_S \left(\sum_{c \in S} |t_c|^2 (1 - \eta_c) \right) + R_S \right]^{n_S} \\
&+ \frac{(-1)^{c_S-1}}{1!} \sum_{a \in S^D} \left[\prod_{b \in S \setminus \{a\}} (1 - d_b) \right] \\
&\times \left[T_S \left(|t_a|^2 \eta_a + \sum_{c \in S \setminus \{a\}} |t_c|^2 (1 - \eta_c) \right) + R_S \right]^{n_S} + \dots \\
&+ \left[\prod_{b \in S \setminus S^D} (1 - d_b) \right] \\
&\times \left[T_S \left(\sum_{c \in S^D} |t_c|^2 + \sum_{c \in S \setminus S^D} |t_c|^2 (1 - \eta_c) \right) + R_S \right]^{n_S}, \\
K_{I, I^D}(n_I) &= (-1)^{c_I} \left[\prod_{b \in I} (1 - d_b) \right] \\
&\times \left[T_I \left(\sum_{c \in I} |t_c|^2 (1 - \eta_c) \right) + R_I \right]^{n_I} \\
&+ \frac{(-1)^{c_I-1}}{1!} \sum_{a \in I^D} \left[\prod_{b \in I \setminus \{a\}} (1 - d_b) \right] \\
&\times \left[T_I \left(|t_a|^2 \eta_a + \sum_{c \in I \setminus \{a\}} |t_c|^2 (1 - \eta_c) \right) + R_I \right]^{n_I} + \dots \\
&+ \left[\prod_{b \in I \setminus I^D} (1 - d_b) \right] \\
&\times \left[T_I \left(\sum_{c \in I^D} |t_c|^2 + \sum_{c \in I \setminus I^D} |t_c|^2 (1 - \eta_c) \right) + R_I \right]^{n_I}. \tag{6}
\end{aligned}$$

We now consider symmetric multiports ($t_{S_1} = t_{S_2} = \dots = t_{S_{N_S}} = t_S$, $t_{I_1} = t_{I_2} = \dots = t_{I_{N_I}} = t_I$) and detectors having the same characteristics in the signal and idler fields ($\eta_{S_1} = \eta_{S_2} = \dots = \eta_{S_{N_S}} = \eta_S$, $d_{S_1} = d_{S_2} = \dots = d_{S_{N_S}} = d_S$, $\eta_{I_1} = \eta_{I_2} = \dots = \eta_{I_{N_I}} = \eta_I$, $d_{I_1} = d_{I_2} = \dots = d_{I_{N_I}} = d_I$). Then the probability $f^{N_S, N_I}(c_S, c_I)$ of

having c_S detections somewhere at N_S signal detectors and c_I detections somewhere at N_I idler detectors can be expressed as:

$$f^{N_S, N_I}(c_S, c_I) = \binom{N_S}{c_S} \binom{N_I}{c_I} C_{S^D, I^D}. \tag{7}$$

Using the expression for C_{S^D, I^D} in Eq. (6) we arrive at the relation:

$$\begin{aligned}
f^{N_S, N_I}(c_S, c_I) &= \sum_{n_S=0}^{\infty} \sum_{n_I=0}^{\infty} p(n_S, n_I) \\
&\times K^{S, N_S}(c_S, n_S) K^{I, N_I}(c_I, n_I), \tag{8}
\end{aligned}$$

where

$$\begin{aligned}
K^{i, N_i}(c_i, n_i) &= \binom{N_i}{c_i} (1 - d_i)^{N_i} (1 - T_i \eta_i)^{n_i} (-1)^{n_i} \\
&\times \sum_{l=0}^{c_i} \binom{c_i}{l} \frac{(-1)^l}{(1 - d_i)^l} \left(1 + \frac{l}{N_i} \frac{T_i \eta_i}{1 - T_i \eta_i} \right)^{n_i}, \\
& \quad i = S, I. \tag{9}
\end{aligned}$$

If the number of photons detected by an intensified CCD camera is much lower than the number of pixels detecting the field with a nonnegligible probability, the limits $N_S \rightarrow \infty$ and $N_I \rightarrow \infty$ are appropriate. When determining these limits, the overall noise levels D_S and D_I are held to be constant ($D_S = N_S d_S$, $D_I = N_I d_I$). The coefficients K defined in Eq. (9) then simplify:

$$\begin{aligned}
K^{i, \infty}(c_i, n_i) &= \sum_{l=0}^{\min(c_i, n_i)} \binom{n_i}{l} (T_i \eta_i)^l (1 - T_i \eta_i)^{n_i - l} \\
&\times \frac{D_i^{c_i - l}}{(c_i - l)!} \exp(-D_i), \quad i = S, I. \tag{10}
\end{aligned}$$

III. RECONSTRUCTION OF THE JOINT SIGNAL-IDLER PHOTON-NUMBER DISTRIBUTION

The probabilities (frequencies) $f^{\infty, \infty}(c_S, c_I)$ are measured and the relation in Eq. (8) then has to be inverted in order to obtain the joint signal-idler photon-number distribution $p(n_S, n_I)$. The relation in Eq. (8) together with the coefficients $K^{i, \infty}(c_i, n_i)$ defined in Eq. (10) can be inverted under special conditions analytically. For instance, if $D_S = D_I = 0$ the inversion relation is found using ‘‘convolution’’ of $f^{\infty, \infty}$ with the Bernoulli distributions with efficiencies $1/(T_S \eta_S)$ and $1/(T_I \eta_I)$. However, analytical approaches are not suitable for processing real experimental data [18]. Reconstruction algorithms have occurred to be suitable in this case [14]. Such algorithms are able to find a joint signal-idler photon-number distribution $\rho^{(\infty)}(n_S, n_I)$ that gives the measured frequencies $f^{\infty, \infty}(c_S, c_I)$ with the highest probability from

all possible photon-number distributions. We use the Kullback-Leibler divergence as a measure of distance between the experimental data and results provided by the developed theory. The joint signal-idler photon-number distribution $\rho^{(\infty)}(n_S, n_I)$ that minimizes the Kullback-Leibler divergence may be found, e.g., using the iterative Expectation-Maximization algorithm [19,20]:

$$\rho^{(n+1)}(n_S, n_I) = \rho^{(n)}(n_S, n_I) \times \sum_{i_S, i_I=0}^{\infty} \frac{f^{\infty, \infty}(i_S, i_I) K^{S, \infty}(i_S, n_S) K^{I, \infty}(i_I, n_I)}{\sum_{j_S, j_I=0}^{\infty} K^{S, \infty}(i_S, j_S) K^{I, \infty}(i_I, j_I) \rho^{(n)}(j_S, j_I)}. \quad (11)$$

The symbol $\rho^{(n)}(n_S, n_I)$ denotes the joint signal-idler photon-number distribution after the n -th step of iteration, $\rho^{(0)}(n_S, n_I)$ is an arbitrary initial photon-number distribution.

Experimental setup used for the measurement of frequencies $f^{\infty, \infty}(c_S, c_I)$ is shown in Fig. 2.

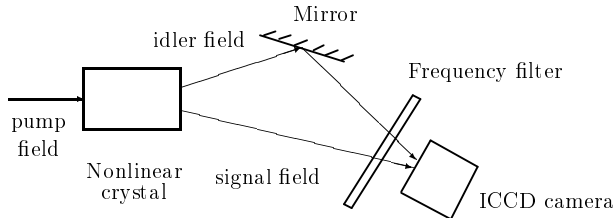


FIG. 2. Scheme of the setup for detection of photon pairs. Fields composed of typically tens of photon pairs are generated in a nonlinear crystal, then they propagate through a frequency filter and are detected on an intensified single-photon CCD camera.

Photon pairs are generated in a 5 mm long LiIO_3 crystal pumped by intense ultrashort pulses delivered by a titanium-sapphire femtosecond laser followed by a regenerative amplifier at the wavelength of 800 nm. The laser system runs at the repetition rate of 11 kHz and after converting the 800-nm beam to its second harmonic it typically delivers pulses with the energy of 0.1 μJ . Photons in the idler field are reflected from a high-reflectivity mirror and impinge on an intensified CCD camera. Signal photons come directly to the photocathode of the intensified camera. Three regions of interest are defined in the field of view of the camera: the first one is for the signal field, the second one for the idler field, and the third region serves for reference measurements of the noise level. The whole field of the camera is filtered by a high-transmittance high-pass filter blocking light below 700 nm and by an interference filter of 10 nm FWHM centered at 800 nm. The interference filter selects nearly degenerate photon pairs. A typical histogram of the measured frequencies of the joint signal-idler photon-number distribution $f^{\infty, \infty}(c_S, c_I)$ is shown in Fig. 3.

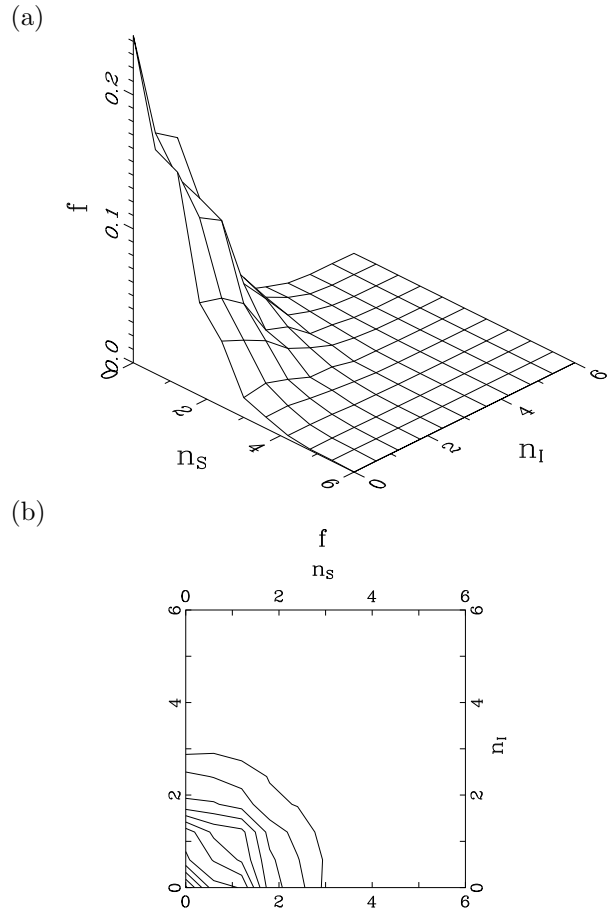


FIG. 3. (a) Measured histogram of the frequencies $f^{\infty, \infty}$ as a function of the signal (n_S) and idler (n_I) photon numbers. (b) Topological graph of the histogram $f^{\infty, \infty}$.

The reconstruction algorithm in Eq. (11) lead to the joint signal-idler photon-number distribution $\rho^{(\infty)}(n_S, n_I)$ in the output plane of the crystal as shown in Fig. 4. We have assumed $T_S \eta_S = T_I \eta_I = 0.03$ after taking into account losses in the setup (frequency filters, reflection on the output plane of the crystal, final quantum efficiency of the intensified CCD camera). The measurement has also provided values of noises; $D_S = D_I = 0.1$. The initial joint signal-idler photon-number distribution $\rho^{(0)}$ was assumed to be uniform.

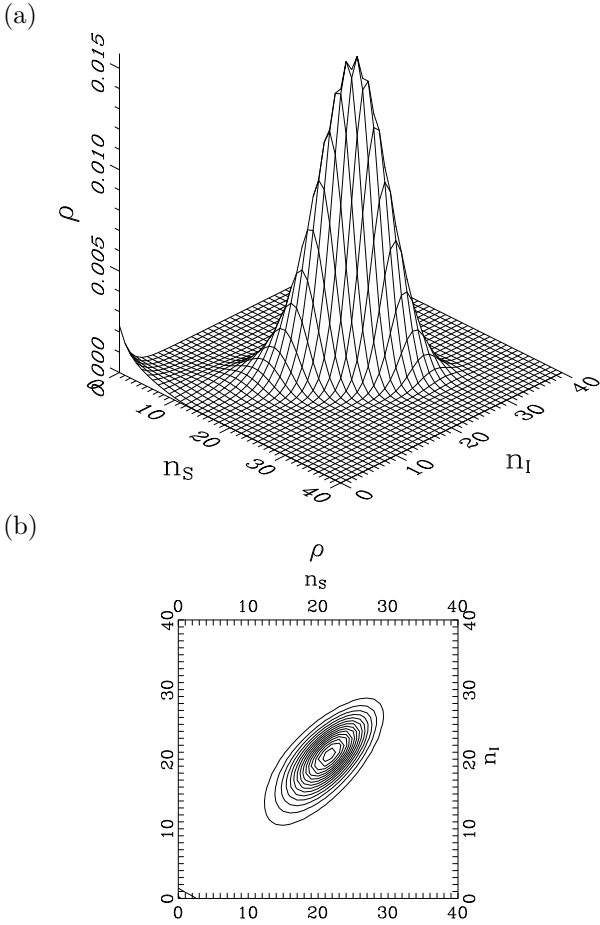


FIG. 4. (a) Reconstructed joint signal-idler photon-number distribution $\rho^{(\infty)}$ as a function of the signal (n_S) and idler (n_I) photon numbers. (b) Topological graph of the distribution $\rho^{(\infty)}$.

The graph in Fig. 4 clearly shows that signal and idler photons are generated in pairs to some extent. In order to quantify this property we use covariance C_p of two stochastic signals n_1 and n_2 described by a joint probability distribution $p(n_1, n_2)$:

$$C_p = \frac{\langle \Delta n_1 \Delta n_2 \rangle}{\sqrt{\langle (\Delta n_1)^2 \rangle \langle (\Delta n_2)^2 \rangle}}, \quad (12)$$

$$\Delta n_i = n_i - \langle n_i \rangle, i = 1, 2,$$

$$\langle n_1 n_2 \rangle = \sum_{n_1=0}^{\infty} \sum_{n_2=0}^{\infty} n_1 n_2 p(n_1, n_2),$$

$$\langle n_i^m \rangle = \sum_{n_1=0}^{\infty} \sum_{n_2=0}^{\infty} n_i^m p(n_1, n_2), i = 1, 2, m = 1, 2.$$

Covariance C_f of the measured distribution $f^{\infty, \infty}$ equals 0.025 in our experiment. This value of C_f is in agreement with the theoretical value determined along the model developed in Sec. 2 for values of parameters defined above. The obtained low value of C_f shows that photons from photon pairs are lost with a high probability owing to low detection efficiencies. However, covariance C_p of the

reconstructed joint signal-idler photon-number distribution $\rho^{(\infty)}$ equals 0.81. This means, that the reconstruction algorithm is able to reveal clearly the original pairing of photons. We note that we have checked that the reconstruction algorithm cannot give correlations of signals being independent (i.e. with no correlation) in the input to this algorithm. Independent simulation data provided by the theoretical model in Sec. 2 were used for this purpose. There are two reasons why the value of C_p characterizing the reconstructed photon-number distribution $\rho^{(\infty)}$ does not approach value 1. Impossibility of the developed model to describe precisely all noises occurring in the experiment represents the first reason. The second reason lies in the fact that the numerical implementation of the reconstruction algorithm loses its precision with the increasing number of iterations.

Pairing of the signal and idler photons results in narrowing of the distribution $\rho_-^{(\infty)}$ of the difference $n_S - n_I$ of the signal and idler photon numbers. Figure 5 shows the distribution $\rho_-^{(\infty)}$ determined from the reconstructed $\rho^{(\infty)}(n_S, n_I)$ and compares it with the distribution ρ_-^{indep} characterizing independent marginal signal and idler distributions:

$$\rho_-^{(\infty)}(n) = \sum_{n_S=0}^{\infty} \sum_{n_I=0}^{\infty} \delta_{n, n_S - n_I} \rho^{(\infty)}(n_S, n_I),$$

$$\rho_-^{\text{indep}}(n) = \sum_{n_S=0}^{\infty} \sum_{n_I=0}^{\infty} \delta_{n, n_S - n_I} \rho_S^{(\infty)}(n_S) \rho_I^{(\infty)}(n_I), \quad (13)$$

and

$$\rho_S^{(\infty)}(n_S) = \sum_{n_I=0}^{\infty} \rho^{(\infty)}(n_S, n_I),$$

$$\rho_I^{(\infty)}(n_I) = \sum_{n_S=0}^{\infty} \rho^{(\infty)}(n_S, n_I). \quad (14)$$

The symbol δ stands for Kronecker delta.

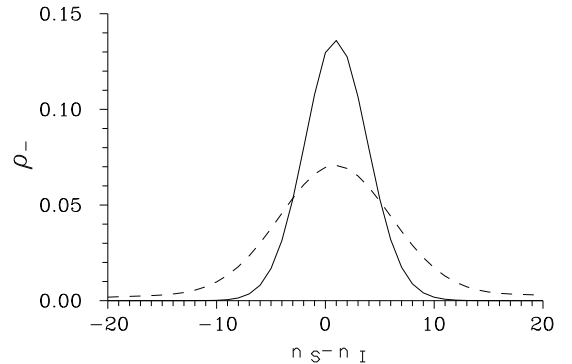


FIG. 5. Distributions $\rho_-^{(\infty)}$ (solid curve) and ρ_-^{indep} (dashed curve) of the difference $n_S - n_I$ of the signal and idler photon numbers.

We note that narrowing of the distribution $\rho_-^{(\infty)}$ has been observed for stronger fields generated by parametric downconversion in a resonator utilizing correlations of photocurrents from two detectors [21].

Narrowing of the distribution $\rho_-^{(\infty)}$ is accompanied by broadening of the distribution $\rho_+^{(\infty)}$ for the sum $n_S + n_I$:

$$\rho_+^{(\infty)}(n) = \sum_{n_S=0}^{\infty} \sum_{n_I=0}^{\infty} \delta_{n, n_S+n_I} \rho^{(\infty)}(n_S, n_I). \quad (15)$$

This stems from the following expression for the variances $\langle [\Delta(n_S - n_I)]^2 \rangle$ and $\langle [\Delta(n_S + n_I)]^2 \rangle$:

$$\langle [\Delta(n_S \pm n_I)]^2 \rangle = \langle (\Delta n_S)^2 \rangle + \langle (\Delta n_I)^2 \rangle \pm 2\sqrt{\langle (\Delta n_S)^2 \rangle \langle (\Delta n_I)^2 \rangle} C_\rho; \quad (16)$$

covariance C_ρ is given in Eq. (12). Figure 6 shows the distribution $\rho_+^{(\infty)}$ derived from the reconstructed data together with the distribution ρ_+^{indep} determined from the independent distributions $\rho_S^{(\infty)}$ and $\rho_I^{(\infty)}$ (14):

$$\rho_+^{\text{indep}}(n) = \sum_{n_S=0}^{\infty} \sum_{n_I=0}^{\infty} \delta_{n, n_S+n_I} \rho_S^{(\infty)}(n_S) \rho_I^{(\infty)}(n_I). \quad (17)$$

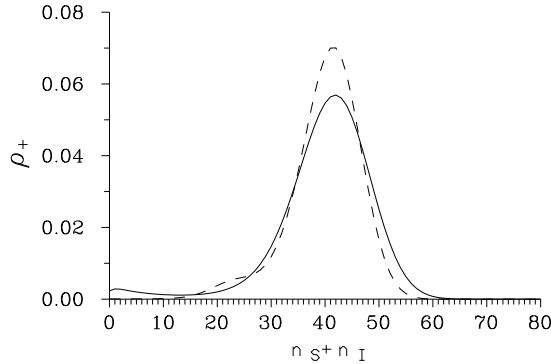


FIG. 6. Distributions $\rho_+^{(\infty)}$ (solid curve) and ρ_+^{indep} (dashed curve) of the sum $n_S + n_I$ of the signal and idler photon numbers.

Statistics of generated photon pairs as they occur in the output plane of the crystal cannot be inferred directly from values of diagonal elements of the reconstructed joint signal-idler photon-number distribution $\rho^{(\infty)}$ in Eq. (11) because of its blurring. This statistics can be determined from the marginal photon-number distributions $\rho_S^{(\infty)}$ and $\rho_I^{(\infty)}$ or from the photon-number distribution of the mixed signal and idler field $\rho_+^{(\infty)}$. Statistics are then judged according to the value of the coefficient S_p ,

$$S_p = \frac{\langle n^2 \rangle}{\langle n \rangle^2} - \frac{1}{\langle n \rangle}, \quad (18)$$

$$\langle n^k \rangle = \sum_{n=0}^{\infty} n^k p(n), k = 1, 2;$$

$S_p = 0$ characterizes Poissonian statistics whereas $S_p = 1$ stands for Gaussian statistics. The values $S_{f,S} = 1.001$, $S_{f,I} = 1.007$, and $S_{f,+} = 1.019$ characterize the directly measured distribution $f^{(\infty, \infty)}$. The reconstructed distribution $\rho^{(\infty)}$ is characterized by the values $S_{\rho,S} = 1.003$, $S_{\rho,I} = 1.013$, and $S_{\rho,+} = 1.027$.

Assuming Poissonian statistics of photon pairs, i.e. $p(n_S, n_I) = \delta_{n_S, n_I} \mu^{n_S} \exp(-\mu) / n_S!$, the theoretical model gives for $\mu = 20$ $S_{p,S} = 1$, $S_{p,I} = 1$, $S_{p,+} = 1.025$ in the output plane of the crystal, whereas $S_{f,S} = 1$, $S_{f,I} = 1$, $S_{f,+} = 1.017$ are appropriate for distributions detected by an intensified CCD camera. On the other hand, Gaussian photon-pair statistics, $p(n_S, n_I) = \delta_{n_S, n_I} \mu^{n_S} / (\mu+1)^{n_S+1}$, used in the theoretical model with $\mu = 20$, give $S_{p,S} = 2$, $S_{p,I} = 2$, $S_{p,+} = 2$ in the output plane of the crystal and $S_{f,S} = 1.69$, $S_{f,I} = 1.69$, $S_{f,+} = 1.71$ for distributions detected by an intensified CCD camera. Comparison of these theoretical results with the above ones stemming from experiment and reconstruction clearly shows that photon pairs are generated with Poissonian statistics.

Poissonian statistics correspond to the physical picture in which photon pairs can be generated into a great number of independent modes distinguishable in space and time (see Appendix A). In case of our experimentally generated fields containing typically several tens of photon pairs, each pair occupies its own mode with a high probability. If photon pairs are generated into one well-defined space-time mode, statistics of photon pairs would be Gaussian (see Appendix A).

IV. JOINT SIGNAL-IDLER INTEGRATED-INTENSITY DISTRIBUTION

A complete characterisation of the generated signal and idler fields is given by the joint distribution of their integrated intensities W_S and W_I in the output plane of the crystal;

$$\hat{W}_l = \int_{-\infty}^{\infty} d\tau \hat{E}_l^{(-)}(\tau) \hat{E}_l^{(+)}(\tau), \quad l = S, I. \quad (19)$$

The operator amplitudes $\hat{E}_l^{(+)}$ and $\hat{E}_l^{(-)}$ in Eq. (19) are given by Eq. (A5) in Appendix A. Integration over time variable in Eq. (19) is carried out over the field generated by one pump pulse.

Inverting the photodetection equation the joint signal-idler integrated-intensity distribution $P(W_S, W_I, s)$ related to s -ordering of field operators can be determined using the joint signal-idler photon-number distribution $\rho^{(\infty)}$ as ([22], chap. 4):

$$P(W_S, W_I, s) = \frac{4}{(1-s)^2} \exp \left[-\frac{2(W_S + W_I)}{1-s} \right] \times \sum_{n_S=0}^{\infty} \sum_{n_I=0}^{\infty} \frac{\rho^{(\infty)}(n_S, n_I)}{n_S! n_I!} \left(\frac{s+1}{s-1} \right)^{n_S+n_I}$$

$$\times L_{n_S}^0 \left(\frac{4W_S}{1-s^2} \right) L_{n_I}^0 \left(\frac{4W_I}{1-s^2} \right); \quad (20)$$

L_n^0 are Laguerre polynomials. The parameter s equals -1, 0, and 1 for antinormal, symmetric, and normal ordering of field operators, respectively. The integrated-intensity distribution related to normal ordering does not include noise from vacuum fluctuations and that is why it shows all features of the generated fields in their full complexity. However, its structure is rather complex in our case of nonclassical correlated fields (generalized functions are necessary for the description) and that is why we use the distribution related to symmetric ordering. This distribution behaves well and still has the capability to resolve nonclassical properties of the fields by its negative values.

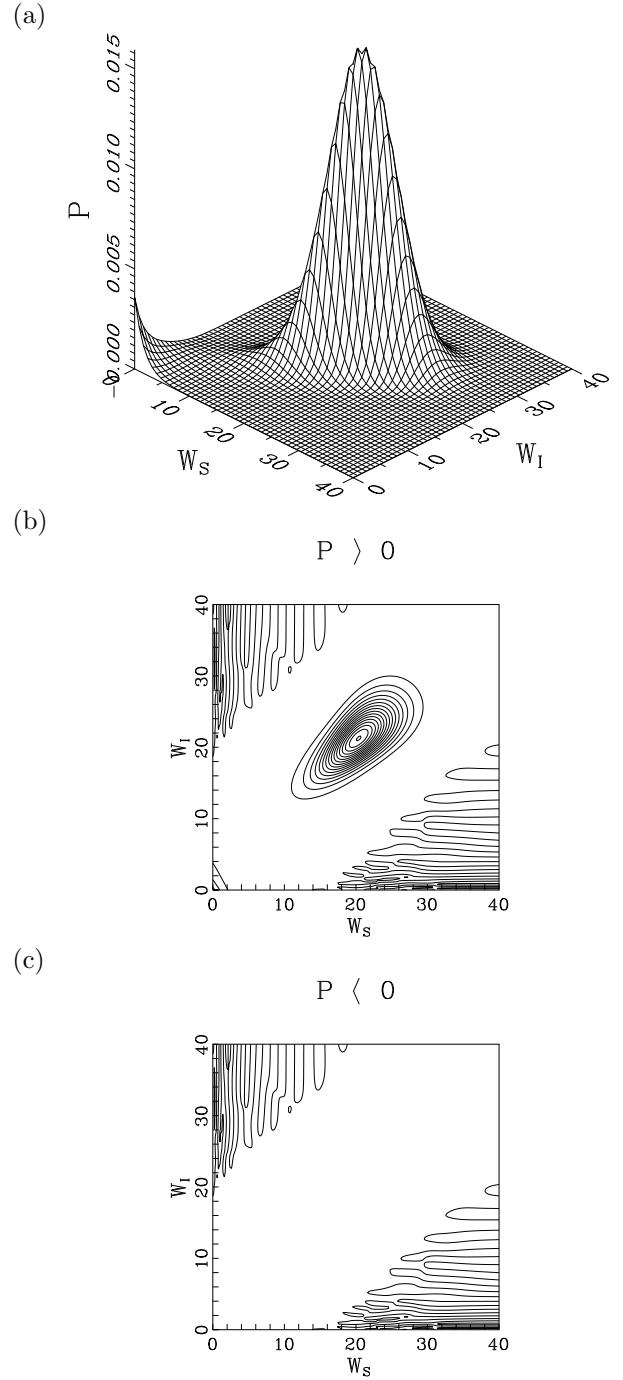


FIG. 7. Joint signal-idler integrated-intensity distribution $P(W_S, W_I, 0)$, (a) 3D plot, (b) topological plot showing lines having positive values, and (c) topological plot showing lines having negative values of the integrated intensity for the reconstructed photon-number distribution $\rho^{(\infty)}(n_S, n_I)$.

The signal-idler integrated-intensity distribution $P(W_S, W_I, 0)$ related to symmetric ordering of operators and obtained from the reconstructed signal-idler photon-number distribution $\rho^{(\infty)}$ is shown in Fig. 7. It clearly shows strong correlations in values of the integrated in-

tensities W_S and W_I . This correlation inherent to the fields in the moment of their generation again shows that photons are generated in pairs, i.e., the same number of energy quanta is put into both fields during their generation. Negative values of the distribution $P(W_S, W_I, 0)$ (see Fig. 7c) reached in some regions of values of integrated intensities W_S and W_I mean that the generated signal-idler field with its correlations is nonclassical (i.e., it cannot be described by classical statistical optics). For comparison, Fig. 8 contains the signal-idler integrated-intensity distribution $P(W_S, W_I, 0)$ for an ideally correlated signal-idler field with Poissonian statistics.

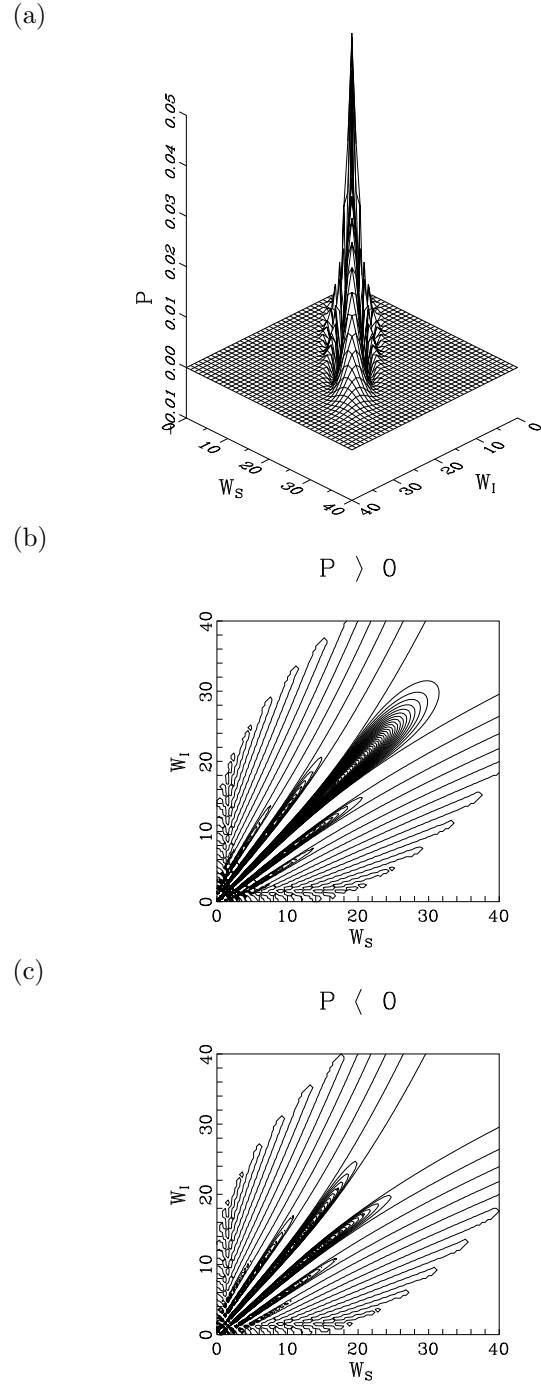


FIG. 8. Joint signal-idler integrated-intensity distribution $P(W_S, W_I, 0)$, (a) 3D plot, (b) topological plot showing lines having positive values, and (c) topological plot showing lines having negative values for $\rho^{(\infty)}(n_S, n_I) = \delta_{n_S, n_I} \mu^{n_S} \exp(-\mu) / n_S!$, $\mu = 20$.

All nonclassical features visible in this distribution in Fig. 8 are contained in the experimentally-obtained distribution shown in Fig. 7.

V. CONCLUSIONS

We have experimentally verified that photons are generated in pairs into the signal and idler fields in the non-linear process of spontaneous parametric downconversion. Both the experimentally determined joint signal-idler photon-number distribution and joint signal-idler integrated-intensity distribution show strong correlations between quantities characterizing the signal and idler fields. For example, covariance of the signal and idler photon numbers is greater than 80 %. Statistics of the generated photon pairs have been determined to be Poissonian. Nonclassical character of the generated signal-idler field manifests itself by negative values of the joint signal-idler integrated-intensity distribution.

ACKNOWLEDGMENTS

The authors thank J. Peřina for helpful discussions. The authors acknowledge the support by the projects Research Center for Optics (LN00A015) and CEZJ-14/98 of the Ministry of Education of the Czech Republic.

APPENDIX A: PHOTON-PAIR STATISTICS IN SPONTANEOUS PARAMETRIC FREQUENCY DOWNCONVERSION FROM FIRST PRINCIPLES

The interaction Hamiltonian \hat{H}_{int} of the process of spontaneous parametric frequency downconversion can be written in the form [1,23,24]:

$$\begin{aligned} \hat{H}_{\text{int}}(t) &= C_{\text{int}} \sum_{k_s} \sum_{k_i} \phi(k_S, k_I, t) \hat{a}_S^\dagger(k_S) \hat{a}_I^\dagger(k_I) + \text{H.c.} \\ &= \hat{H}_{\text{int}}^{(-)}(t) + \hat{H}_{\text{int}}^{(+)}(t), \end{aligned} \quad (\text{A1})$$

where C_{int} is an interaction constant and $\phi(k_S, k_I, t)$ describes a detailed space-time structure of the emitted photon fields. The symbol H.c. denotes Hermitian conjugate. The operator $\hat{H}_{\text{int}}^{(-)}$ ($\hat{H}_{\text{int}}^{(+)}$) stands for the part of the interaction Hamiltonian \hat{H}_{int} containing creation (annihilation) operators of modes in the signal and idler fields.

The state of the signal and idler fields in the output plane of the crystal is obtained solving the Schrödinger equation in the form:

$$\begin{aligned} |\psi\rangle &= \sum_{n=0}^{\infty} |\psi_n\rangle, \\ |\psi_0\rangle &= |\text{vac}\rangle, \\ |\psi_n\rangle &= \left(-\frac{i}{\hbar}\right)^n \int_{-\infty}^{\infty} d\tau_1 \int_{-\infty}^{\tau_1} d\tau_2 \dots \int_{-\infty}^{\tau_{n-1}} d\tau_n \\ &\quad \times \hat{H}_{\text{int}}^{(-)}(\tau_1) \dots \hat{H}_{\text{int}}^{(-)}(\tau_n) |\text{vac}\rangle, \quad n = 1, 2, \dots \end{aligned} \quad (\text{A2})$$

The signal and idler fields are assumed to be in the vacuum state $|\text{vac}\rangle$ in the input plane of the crystal.

If the number of photons in the signal and idler fields is much lower than the number of independent modes constituting these fields, we may approximately write:

$$\begin{aligned} |\psi_n\rangle &\simeq \left(-\frac{i}{\hbar}\right)^n \int_{-\infty}^{\infty} d\tau_1 \int_{-\infty}^{\tau_1} d\tau_2 \dots \int_{-\infty}^{\tau_{n-1}} d\tau_n \\ &\quad \hat{H}_{\text{int}}^{(-)}(\tau_1) \dots \hat{H}_{\text{int}}^{(-)}(\tau_n) |\text{vac}\rangle \\ &= \left(-\frac{i}{\hbar}\right)^n \frac{1}{n!} \left[\int_{-\infty}^{\infty} d\tau \hat{H}_{\text{int}}^{(-)}(\tau) \right]^n |\text{vac}\rangle, \\ &\quad n = 1, 2, \dots \end{aligned} \quad (\text{A3})$$

The state $|\psi_n\rangle$ then describes the field containing just n photon pairs.

Statistics of the generated photon pairs may be inferred from the normally ordered moments of the “creation operator of photon pairs” \hat{P}_{pair} and its Hermitian conjugate:

$$\hat{P}_{\text{pair}}(\tau_S, \tau_I) = \underline{\hat{E}_S^{(-)}(\tau_S)} \underline{\hat{E}_I^{(-)}(\tau_I)}. \quad (\text{A4})$$

The symbol $\hat{E}_l^{(+)}$ ($\hat{E}_l^{(-)}$) denotes the positive- (negative-) frequency part of the electric-field amplitude of the signal ($l = S$) and idler ($l = I$) field:

$$\begin{aligned} \hat{E}_l^{(+)}(\tau) &= \sum_{k_l} e_l(k_l) \hat{a}_l(k_l) \exp(-i\omega_{k_l}\tau), \\ \hat{E}_l^{(-)} &= \left(\hat{E}_l^{(+)}\right)^\dagger; \end{aligned} \quad (\text{A5})$$

$e_l(k_l)$ is a normalization amplitude of the mode k_l , $l = S, I$. Underlining of the operators on the right-hand side of Eq. (A4) means that “only the signal and idler photons created in the same elementary event are considered” (see the expression for $|\psi_n\rangle$ in Eq. (A3)).

We may write for the normally ordered moments of $\hat{P}_{\text{pair}}^\dagger$ and \hat{P}_{pair} in the framework of the above defined approximation:

$$\begin{aligned} \langle \psi_n | &\left[\prod_{j=1}^n \hat{P}_{\text{pair}}^\dagger(\tau_{S_j}, \tau_{I_j}) \right] \\ &\times \left[\prod_{j=1}^n \hat{P}_{\text{pair}}(\tau_{S_{n+1-j}}, \tau_{I_{n+1-j}}) \right] | \psi_n \rangle = \\ &\left[\prod_{j=1}^n \langle \psi_1 | \hat{P}_{\text{pair}}^\dagger(\tau_{S_j}, \tau_{I_j}) | \text{vac} \rangle \right] \\ &\times \left[\prod_{j=1}^n \langle \text{vac} | \hat{P}_{\text{pair}}(\tau_{S_{n+1-j}}, \tau_{I_{n+1-j}}) | \psi_1 \rangle \right] = \\ &\prod_{j=1}^n \left| \langle \psi_1 | \hat{P}_{\text{pair}}^\dagger(\tau_{S_j}, \tau_{I_j}) | \text{vac} \rangle \right|^2, \\ &\quad n = 1, 2, \dots \end{aligned} \quad (\text{A6})$$

Assuming $\tau_{S_1} = \tau_{S_2} = \dots = \tau_S$ and $\tau_{I_1} = \tau_{I_2} = \dots = \tau_I$, Eq. (A6) provides a simplified expression:

$$\langle \psi_n | \left[\hat{P}_{\text{pair}}^\dagger(\tau_S, \tau_I) \right]^n \left[\hat{P}_{\text{pair}}(\tau_S, \tau_I) \right]^n | \psi_n \rangle = \left| \langle \psi_1 | \hat{P}_{\text{pair}}^\dagger(\tau_S, \tau_I) | \text{vac} \rangle \right|^{2n}. \quad (\text{A7})$$

Assuming that the contribution from the state $|\psi_n\rangle$ is much greater than those from the states $|\psi_k\rangle$ for $k = n + 1, n + 2, \dots$, the relation in Eq. (A7) implies that statistics of generated photon pairs is Poissonian.

If photon pairs are generated into one well-defined space-time mode, than the positive-frequency part of the electric-field amplitude $\hat{E}_l^{(+)}$ of field l can be written as

$$\hat{E}_l^{(+)}(\tau) = a_l(\tau)\hat{a}_l, \quad (\text{A8})$$

where a_l describes amplitude per photon and \hat{a}_l stands for annihilation operator of a photon in field l ($l = S, I$). We then have:

$$\begin{aligned} \langle \psi_n | \left[\hat{P}_{\text{pair}}^\dagger(\tau_S, \tau_I) \right]^n \left[\hat{P}_{\text{pair}}(\tau_S, \tau_I) \right]^n | \psi_n \rangle &= \\ |a(\tau_S)a(\tau_I)|^{2n} \langle \psi_n | \left[\hat{a}_S^\dagger \hat{a}_I^\dagger \right]^n \left[\hat{a}_S \hat{a}_I \right]^n | \psi_n \rangle &= \\ |a(\tau_S)a(\tau_I)|^{2n} n! = n! \left| \langle \psi_1 | \hat{P}_{\text{pair}}^\dagger(\tau_S, \tau_I) | \text{vac} \rangle \right|^{2n}. \end{aligned} \quad (\text{A9})$$

Relations in Eq. (A9) are in agreement with Gaussian statistics of generated photon pairs.

- [9] R. A. Campos, B. E. A. Saleh, and M. C. Teich, Phys. Rev. A **40**, 1371 (1989).
- [10] P. Törmä, T. Kiss, I. Jex, and H. Paul, Jemná mechanika a optika **11-12**, 338 (1996).
- [11] J. Kim, S. Takeuchi, Y. Yamamoto, and H. H. Hogue, Appl. Phys. Lett. **74**, 902 (1999).
- [12] A. J. Miller, S. W. Nam, J. M. Martinis, and A. V. Sergienko, Appl. Phys. Lett. **83**, 791 (2003).
- [13] S. Brattke, B. T. H. Varcoe, and H. Walther, Phys. Rev. Lett. **86**, 3534 (2001).
- [14] J. Řeháček, Z. Hradil, O. Haderka, J. Peřina Jr., and M. Hamar, Phys. Rev. A **67**, 061801(R) (2003).
- [15] D. Achilles, Ch. Silberhorn, C. Sliwa, K. Banaszek, and I. A. Walmsley, quant-ph/0305191.
- [16] M. J. Fitch, B. C. Jacobs, T. B. Pittman, and J. D. Franson, quant-ph/0305193.
- [17] B. M. Jost, A. V. Sergienko, A. F. Abouraddy, B. E. A. Saleh, and M. C. Teich, Opt. Express **3**, 81 (1998).
- [18] D. Mogilevtsev, Z. Hradil, and J. Peřina, J. Mod. Opt. **44**, 2261 (1997).
- [19] A. P. Dempster, N. M. Laird, and D. B. Rubin, J. R. Statist. Soc. B **39**, 1 (1977).
- [20] Y. Vardi and D. Lee, J. R. Statist. Soc. B **55**, 569 (1993).
- [21] Y. Zhang, K. Kasai, and M. Watanabe, Opt. Lett. **27**, 1244 (2002).
- [22] J. Peřina, *Quantum Statistics of Linear and Nonlinear Optical Phenomena* (Kluwer, Dordrecht, 1991), 2nd edition.
- [23] J. Peřina Jr., A. V. Sergienko, B. M. Jost, B. E. A. Saleh, and M. C. Teich, Phys. Rev. A **59**, 2359 (1999).
- [24] J. Peřina Jr., Eur. Phys. J. D **7**, 235 (1999).

-
- [1] L. Mandel and E. Wolf, *Optical Coherence and Quantum Optics* (Cambridge University Press, Cambridge, 1995), chap. 22.4.
 - [2] D. F. Walls and G. J. Milburn, *Quantum Optics* (Springer, Berlin, 1995), chap. 5.
 - [3] J. Peřina, Z. Hradil, and B. Jurčo, *Quantum Optics and Fundamentals of Physics* (Kluwer, Dordrecht, 1994), chap. 8.
 - [4] S. Ranzilli, W. Tittel, H. De Riedmatten, H. Zbinden, P. Baldi, M. De Micheli, D. B. Ostrowsky, and N. Gisin, Eur. Phys. J. D. **18**, 155 (2002).
 - [5] T. S. Larchuk, M. C. Teich, and B. E. A. Saleh, Annals of the New York Academy of Sciences **755**, 680 (1995).
 - [6] J. Peřina Jr., O. Haderka, and J. Soubusta, Phys. Rev. A **64** (2001) 052305.
 - [7] O. Haderka and J. Peřina Jr., in *Decoherence and its Applications in Quantum Computation and Information Transfer, NATO Science Series, Series III: Computer and System Sciences Vol. 182*, edited by T. Gonis and P. E. A. Turchi, (IOP Press, Amsterdam, 2001). p. 186.
 - [8] O. Haderka and J. Peřina Jr., in *Wave and Quantum Aspects of Contemporary Optics, Proc. SPIE Vol. 4356*, edited by J. Peřina, M. Hrabovský, and J. Křepelka (SPIE, Bellingham, 2001), p. 61.